ARTICLE NO. 78-661R

The MPD Thruster Test on the Space Shuttle

Kyoichi Kuriki*
University of Tokyo, Komaba, Tokyo, Japan

A magnetoplasmadynamic arcjet is scheduled to be on board the first Spacelab to perform space experiments with particle accelerators. Major scientific missions to be carried out by the arcjet are 1) spacecraft charge neutralization with an electron gun simultaneously operated, 2) plasmadynamics in the background geomagnetic field, and 3) excitation of artificial airglow. Space-chamber tests were carried out twice, in Dec. 1976 and Nov. 1977. The results of these tests as well as the hardware design are presented.

Introduction

DURING the last decade a large number of ionospheric experiments have been made by satellites and sounding rockets. Most of the data were obtained by passive observations. Information from active experiments has been expected to reveal the cause and effect of ionospheric phenomena such as auroral and airglow excitations. Active experiments are intended to inject particle beams into the ionosphere and to observe the wave excitation as well as the particle interaction with ionospheric constituents and the geomagnetic field. The Space Shuttle inaugurates a new era for these experiments with its advantage of high power capability and the attendance of payload specialists.

As an active experiment, SEPAC (Space Experiments with Particle Accelerators) is scheduled to be carried out on Spacelab 1 in June 1981.[1] The SEPAC instrument system consists of a 2 kJ quasisteady magnetoplasmadynamic (MPD) arcjet, a 10 kW (7.5 kV, 1.3 A) electron beam accelerator, a diagnostic probe package, and a control and data management subsystem. The MPD arcjet has been developed as an electric thruster.[2-4] The discharge chamber of the MPD arcjet consists of coaxial electrodes and propellant inlet ports. There the propellant is ionized and accelerated electromagnetically at high discharge current. For the Spacelab 1 mission, an MPD arcjet was adopted because it can efficiently provide a large number of plasma particles, and is safely operated at voltages much lower than that of conventional plasma gun. This paper reviews the scientific missions, the hardware designs, and the results of the space-chamber tests associated with the MPD arcjet.

Scientific Mission

The major scientific objectives of SEPAC are described in the following subsections. Those associated with the MPD arcjet are 1) vehicle charge neutralization, 2) artificial airglow excitation, and 3) plasmadynamics experiment. The first experiment requires simultaneous operation of the electron beam accelerator (EBA) and an MPD arcjet. The objectives mainly related to EBA are 4) beam plasma and wave interaction, 5) auroral excitation, and 6) electron echo experiment (E and B field morphology). The latter three experiments are difficult to carry out by EBA alone, because of the charging problem, and require the simultaneous operation of either an MPD arcjet or a neutral gas jet. The first experiment alone has a technological aspect. So far, the performance test of the MPD arcjet as a thruster is not scheduled, except for the acquisition of discharge characteristics data. The first three experiments are discussed in detail.

Vehicle Charge Neutralization

When an electron beam is injected into the ionosphere from EBA, a positive charge builds up on the Shuttle to which the EBA is grounded. The capacitance of the Space Shuttle is a few hundreds of picofarads. Supposing an electric charge of 1 C (1 A×1 s) is removed from the Shuttle to infinity, a positive potential of 10^9 V appears on the Space Shuttle. If the initial beam energy is not high enough, the electron beam is attracted back to the spacecraft within a period much shorter than 1 s. In order to maintain steady beam ejection, the return current must be supplied from the ambient plasma.[5] Since the amount of the return current depends on the turbulent plasma conductivity,[6,7] the charge neutralization is an important problem of plasma physics and, at the same time, it is one of the major SEPAC objectives.

A similar charging problem has occurred with satellites, and arcing phenomena have been studied.[8,9] Further studies are under way on the SCATHA (Spacecraft Charging at High Altitude) satellite launched in Jan. 1979.[10] Although the polarity of satellite charging is contrary to that of the beam ejection experiment, they share the underlying physics. The general guidelines for the establishment of charge neutralization are: 1) the emitting current is balanced by the return current, and no charge accumulation is promoted; 2) the potential distribution of the spacecraft and its surrounding is uniform with no strong electric field; and 3) the spacecraft potential with respect to that of space plasma is sufficiently low. The second condition is necessary to prevent surface arcing and sputtering. The third is the condition for the absence of the bombardment of the particles accelerated over long distance.

In the ionosphere at 250-km altitude where the Space Shuttle flies, the following electron flux is expected as a return current:

$$j_e = en_e v_e/4 \simeq 10^{-3} \quad \mathrm{A/m^2} \tag{1}$$

where the electron density $n_e = 10^5$ cm^{-3} and the electron thermal velocity v_e is calculated for the temperature 2000 K. Since the electrically conducting area of the Space Shuttle is limited to 60 m^2, only 60 mA return current is obtained by the ionospheric electrons. If other contributions, such as the neutral gas ionization by electron beam and the ionization by secondary electron, are taken into account, a slightly larger

Presented as Paper 78-661 at the AIAA/DGLR 13th International Electric Propulsion Conference, San Diego, Calif., April 25-27, 1978; submitted June 12, 1978; revision received May 1, 1979.

Index categories: Atmospheric and Space Sciences; Plasma Dynamics and MHD; Electric and Advanced Space Propulsion.

*Associate Professor, Institute of Space and Aeronautical Science. Member AIAA.

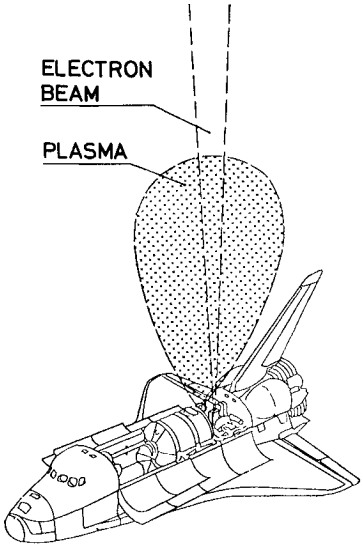

Fig. 1 Vehicle charge neutralization.

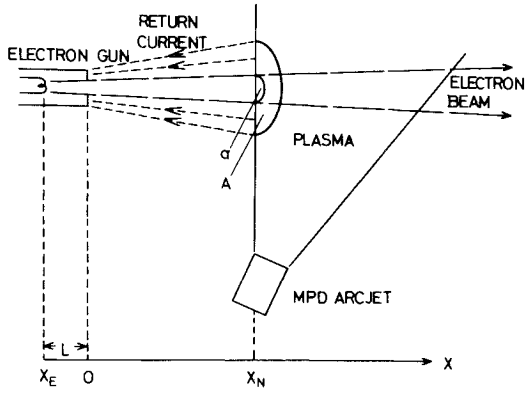

Fig. 2 Schematic of beam-plasma coupling.

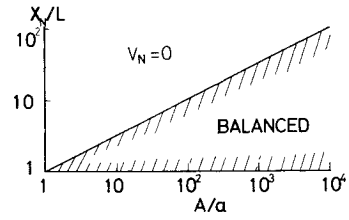

Fig. 3 Current balance condition.

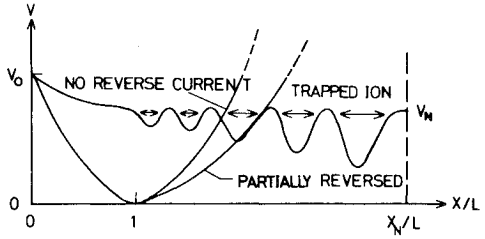

Fig. 4 Potential distributions with and without reverse current.

current results. This current is not yet large enough to sustain the beam current exceeding 1 A. In the SEPAC experiment, therefore, an active neutralization is required. As sketched in Fig. 1, the plasma generated by the MPD arcjet is used as a low-energy electron source for the return current.

The SEPAC quasisteady MPD arcjet generates about 10^{19} electron-ion pairs per shot, which nearly correspond to 1 C of positive and negative charges. A part of these electrons is attracted back to the spacecraft as the return current, while most of the ions escape. Fig. 2 shows the schematic of beam-plasma coupling. The return current is assumed to flow in the annular region outside the electron beam. The return current is limited by 1) the electron emissivity at the plasma surface, and 2) the space charge effect. When the latter effect is dominant and the beam current is balanced by the return current, the following equation results:

$$\frac{a}{A}=\left(\frac{L}{X_N}\right)^2\left(1-\frac{V_N}{V_0}\right)^{3/2} \tag{2}$$

where a and A are areas of the beam cross section and the plasma surface, respectively, and V_N and X_N are plasma potential and location measured from the electron gun exit, respectively. The electrode separation of electron gun is L, as shown in Fig. 2, and V_0 is the acceleration voltage. The current balance condition for $V_N=0$ is satisfied when parameters lie in the shadowed region in Fig. 3. For example when $L=5$ cm, $X_N=5$ m, and the beam diameter is 10 cm, a plasma diameter of more than 10 m is required.

Supposing the current balance condition is satisfied, we have to consider how the plasma lifetime or the neutralization time is determined. The plasma is regarded as an effective electron source as long as it exists in the geomagnetic tube crossing the metal surface of the Shuttle. Bohm diffusion across the magnetic lines of force is a loss mechanism. The diffusion equation for the number density n in the cylindrical coordinate system is given by

$$\frac{\partial n}{\partial t}=D_B\left(\frac{\partial^2 n}{\partial r^2}+\frac{1}{r}\frac{\partial n}{\partial r}\right)$$

$$D_B=\alpha r_{ce} v_e$$

$$\alpha\simeq 0.1 \tag{3}$$

where r_{ce} and v_e are the electron Larmor radius and thermal speed, respectively. This equation was solved with an initial gaussian distribution of 5 m half-value radius and 10^9 cm^{-3} maximum density. The neutralization period was assumed to terminate when the total plasma particles are equal to the sum of the diffusion loss and the particles (electrons) collected by the Shuttle as return current. The diffusion loss was overestimated by disregarding the return current. The neutralization time, therefore, was calculated conservatively and found to be 30 ms. The last figure is very close to the result of the space chamber experiment which will be discussed later. This coincidence is rather fortuitous since the magnetic lines of force are connected to the chamber wall, where the plasma particles are lost in a period much shorter than 30 ms by the surface recombination. Therefore, the effect of trapped ions must be taken into account as follows.

The plasma from the MPD arcjet serves not only as the electron source but also as the ion source which suppresses the space charge effect. It has been known from the one-dimensional analysis of ion engine neutralization that the unneutralized beam cannot proceed steadily beyond $2L$ from the engine exit even when the current balance condition is satisfied, as shown in Fig. 4.[11] With ions trapped in potential wells, a one-dimensional electro-hydrodynamic analysis was made. The current associated with back and forth oscillation of the trapped ions is smaller than the beam current by a factor of the square root of the electron-to-ion mass ratio. As a result, a nonlinear wave train appears between the target plasma and the electron gun, and the electron beam can reach the plasma cloud without reflection. The ions trapped in the potential well of the wave train cancel the space charge of the electron beam. The potential profile is shown in Fig. 4. Similar plasma oscillation is found in the neutralizing region of the ion engine. In this case, the wave train has small amplitude,[11] whereas in the present analysis the wave train is

nonlinear and has finite amplitude. Since the ion-neutral and ion-ion mean collision times are longer than the plasma lifetime estimated by Bohm diffusion, the neutralization time is determined by the plasma diffusion loss across the magnetic field. In a similar manner, the space-charge effect in the return current path may be relaxed by the presence of trapped ions. If this is true, Eq. (2) overestimates the necessary area of the plasma.

The energy distribution of returning electrons will be measured by a retarding potential analyzer on the Shuttle pallet. The result may reveal the potential difference between the Shuttle and the neutralizing plasma cloud. Plasma waves generated by beam-plasma interaction will also be monitored by antennas on the pallet.

Airglow Excitation and Plasmadynamics

An argon plasma ejected by the MPD arcjet interacts with the surrounding atmosphere and emits spectral radiation. Possible radiation processes are the oxygen excitations[12]:

$$O(^3P)+e \rightarrow O(^1D)+e\ (-1.97\,eV)$$
$$\downarrow$$
$$O(^3P)+h\nu(6300\ \text{Å})$$

$$O(^3P)+e \rightarrow O(^1S)+e\ (-4.19\,eV)$$
$$\downarrow$$
$$O\ (^3P)+h\nu(5577\ \text{Å})$$

Although N^+ excitation has higher reaction speed than O excitation, N^+ density is much less than O density, and the resulting radiation intensity of N^+ excitation is smaller than that of O excitation. The electron temperature of the argon plasma generated by the MPD arcjet is about 5 eV, and the electrons lose most of their energy after a single collision for $O(^1S)$ excitation and after two collisions for $O(^1D)$ excitation. The excitations are completed within 0.2 s for $O(^1D)$ and 6 s for $O(^1S)$, and thereafter the emissions persist as the afterglow. The lifetimes of the excited states are 148 s for $O(^1D)$ and 0.7 s for $O(^1S)$. If the effect of particle collision is taken into account, the lifetime of $O(^1D)$ is reduced, and its spontaneous emission is quenched. The reduced lifetime of $O(^1D)$ is 8 s at the Shuttle orbit. When the excitation and deexcitation speeds are combined, both 6300-Å and 5577-Å emissions are found to have nearly the same intensities.

At 200 m away from the Shuttle, where magnetoplasmadynamic effects are expected, the plasma density decreases to 5×10^7 cm^{-3} by expansion. We define I_1 as the radiation intensity of the image formed by an F1 lens and I_2 as that on the frontal optics. If we observe the airglow radiation on the Shuttle, the following intensities are estimated.

1) 6300 Å radiation:

$$I_1 = 2\times10^7 \text{ photons/cm}^2\cdot\text{s}$$
$$I_2 = 4\times10^6 \text{ photons/cm}^2\cdot\text{s}$$

2) 5577 Å radiation:

$$I_1 = 8\times10^7 \text{ photons/cm}^2\cdot\text{s}$$
$$I_2 = 1.5\times10^7 \text{ photons/cm}^2\cdot\text{s}$$

These intensities are just observable by a low-light-level TV camera on board the Space Shuttle. The emissions of these spectral lines are also to be monitered by a photometer with different filters on the Shuttle pallet. These airglow radiations will show the plasma flow pattern and visualize plasmadynamic processes as follows.

Two aspects of the magnetoplasmadynamic effects are conceivable. The first is the hydrodynamical disturbance generated in the ionospheric plasma by the piston effect of the arcjet plasma. Even when the expanded plasma has a diameter

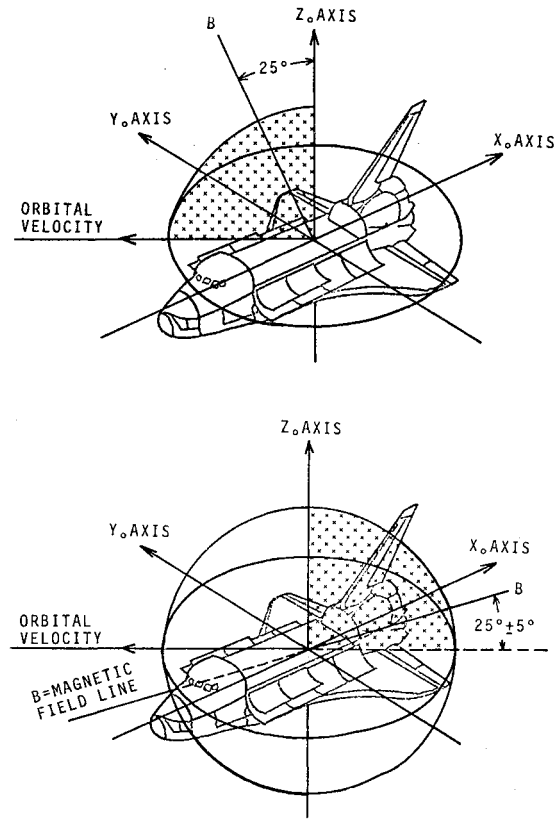

Fig. 5 Shuttle orbiter configurations with respect to magnetic lines of force: a) flow vector parallel to field lines; b) flow vector perpendicular to field lines.

of 1 km, the density is about 10^5 cm^{-3} and is comparable to the background plasma density. The generated disturbance, therefore, results in highly nonlinear effects and may induce shock waves. The waves thus generated are hard to observe by the onboard probes since the waves will propagate mainly away from the Shuttle and generate little optical emission. The second aspect is the reaction of the background geomagnetic field to the plasma flow. At 200 m downstream of jet exit, where the β value of the plasma approaches unity, the plasma flow begins to be guided or retarded by the magnetic field depending on the relative angle between velocity vector and magnetic lines of force.[13]

In order to inject the plasma in parallel with the magnetic lines of force, the Shuttle flies in a configuration shown in Fig. 5a taking the velocities of the plasma and the Shuttle into account. At about 200-m downstream of the arcjet exit, the lateral expansion of the plasma is suppressed by the magnetic field. Inside the plasma flow, an oblique whistler wave propagates towards the centerline, and will probably deform into a collision-free shock wave if the disturbance is strong enough.[14] The ion mean-free-path, which is about 1 km, is much longer than the length under consideration. The wave length relevant to the collision-free shock wave is $10c/\omega_{pe}-c/\omega_{pi} = 10$–$300$ m where c is the light speed, and ω_{pe} and ω_{pi} are electron and ion plasma frequencies, respectively.[15]

The second configuration shown in Fig. 5b is for plasma injection perpendicular to the magnetic field. Since the self-polarization condition $m_i n/\epsilon B^2 \gg 1$ is satisfied, the plasma can flow without deceleration by the magnetic field as far as the classical theory is concerned, where m_i is the ion mass and ϵ is the permittivity.[16] However, if a turbulent conductivity is taken into account, the polarization is destroyed by the short-circuiting current, and the plasma is decelerated. In this case, a collisionless shock wave is expected to appear nearly perpendicular to the magnetic field. The wave is characterized by

the low frequency whistler mode and has a wave length of $c\delta\theta/\omega_{pi}$, where $\delta\theta$ is a deviation angle from the exact perpendicular configuration.[17]

Arcjet Development

The MPD arcjet consists of the components shown in Fig. 6. Electrical power from the 28 V bus line is fed into CHG (charger unit), where the voltage is stepped up to 480 V. The CAP contains a capacitor bank constructing PFN (pulse forming network) and switching elements. The stored energy is transferred into the MPD-HD (head) upon receiving a discharge command signal from the MPD-IU (interface unit). The MPD-GS (gas supply) consists of a high-pressure vessel filled with argon gas and control valves. The gas is supplied to the MPD-FAV (fast acting valve) reservoir at a regulated pressure. When a current pulse energizes the FAV actuator coil, a gas pulse emerges into the discharge chamber in the MPD-HD. All the command and monitor signals are processed and transferred via MPD-IU to and from the CD unit, respectively. An external view of the MPD arcjet is provided in Fig. 7. The electrical characteristics of the SEPAC MPD arcjet are listed in Table 1.

The impact of capacitor failure is prevented from propagating to other parts by the circuitry design of the PFN. The overload of and back current to the charger unit due to the capacitor failure in the short-circuiting mode are inhibited by a fuse-diode combination. The rush current to a short-circuited capacitor from other charged capacitors, as well as the polarity inversion of electrolytitic capacitor, are also prevented by diodes.[18] All the capacitors are contained in a sealed vessel of 1-atm inner pressure. It was found from the capacitor test that the capacitor was not exploded within the power capability of the SEPAC charger.

The arc discharge circuit is isolated from the charger and the Shuttle ground system before starting the discharge. This precaution is taken so that the current path will not form through the structure or in other payloads on the Shuttle. The metal surface is not exposed within a hemisphere of 0.5 m radius with its center at the jet exit. When the metal surface is exposed to the plasma, a part of the discharge current is likely to flow in the metal, which will cause sputtering. When the MPD arcjet is not operated, the electrode system is grounded to the Shuttle "earth" so that the arcjet components are not affected by the operation of other payloads.

The switching element for the arc discharge is a high-power thyrister. The gate-opening speed of the thyrister is 800 A/μs, fast enough to match with the rise time of the discharge current, 100 μs. In order to speed up the current rise, a resistor is connected in parallel with the arc discharge, and the starting current is held through this resistor until a trigger spark initiates the arc discharge. When the arc discharge is misfired, this resistor serves as an energy dump. With this switching device, the charging voltage does not appear at the arcjet electrodes until a gate signal turns on the thyrister.

The MPD-HD, the discharge chamber, is mechanically separated from the MPD-FAV as shown in Fig. 7. If the FAV is attached to the MPD-HD, the heat generated in the FAV is prevented from dissipating through the structure by the heat generated at the electrodes. The heat-resistive materials are listed in Table 2. The maximum power consumption in the

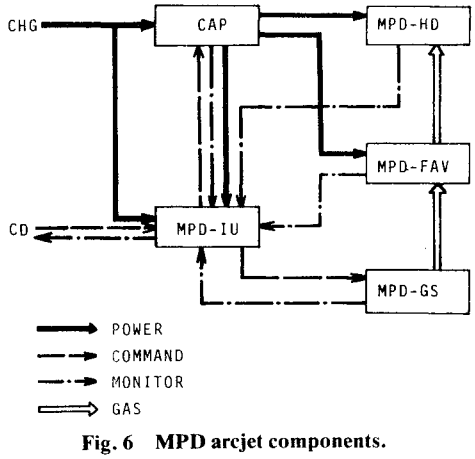

Fig. 6 MPD arcjet components.

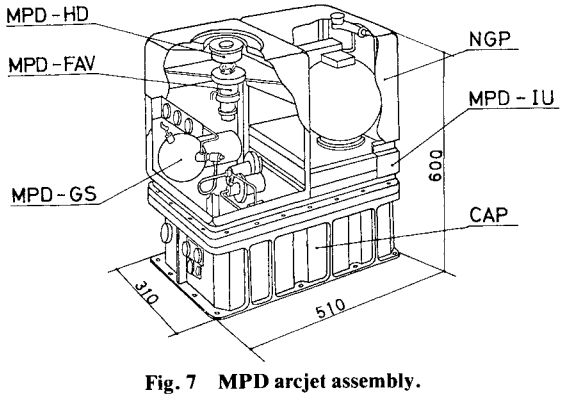

Fig. 7 MPD arcjet assembly.

Table 1 Electrical characteristics of SEPAC MPD arcjet

Arc discharge:	
Stored energy	2 kJ
Voltage	
Charge	480 V
Discharge	240 V
Current	8 kA
Pulse width	1.0 ms
Capacitor (electrolytic)	16,800 μF
PFN section number	4
Characteristic impedance	30 mΩ
FAV driver:	
Voltage (charge)	480 V
Capacitor (electrolytic)	1,200 μF
Trigger discharge:	
Voltage	
Charge	480 V
Output	1.5–2.3 kV
Capacitor (Electrolytic)	220 μF
Pulse width	50 μs

Table 2 Heat-resistive material

Anode, cathode, and trigger pin	Tungsten
Insulator	
Discharge chamber	Boron nitride and alumina ceramic
Electrode mount	FRP
"O" Ring	Silicone compound

Table 3 Mass breakdown of MPD arcjet

Capacitor unit	41.7 kg
Interface unit	3.4 kg
Head	2.0 kg
Fast acting valve	2.0 kg
Gas supply	3.8 kg
Structure	2.5 kg
Total	55.4 kg

MPD arcjet is 630 W, with an average of 200 W. The repetition period of MPD arc firing is limited by the maximum power allocation to SEPAC, 1.6 kW. The arc discharge is repeated every 15 s for 10–15 min. During this period, the temperature of the front panel rises to 100–150°C. Active cooling and heating of the arcjet system rely on the cold plate service of the Spacelab. It is rather important to keep the electrolytic capacitors warm and active since the temperature expected, as low as −150°C in the shadowed pallet, causes permanent damage to the capacitors.

A mass breakdown of the MPD arcjet is shown in Table 3. The mass of the capacitor unit includes that of the sealed container which amounts to 36% of the CAP subtotal. This fraction may be reduced if the stored energy is scaled up.

Space Chamber Test

The plasma ejection tests have been made twice in large space chambers together with the electron beam ejection. The first test was made at NASA Johnson Space Center (JSC) in 1976. The results of the experiments are summarized in Ref. 19. The second test was made at the National Space Development Agency (NASDA) Japan in 1977. The results of this test are now under analysis and will be briefly summarized together with those of JSC experiment.

JSC Experiment

The experiment was carried out in the Large Space Chamber A at JSC, 36.6-m high and 19.8-m in diameter. An MPD arcjet and an electron gun were located on the ground floor, and diagnostic probes such as Langmuir probes and B- and E-field probes were arranged along beam and plasma passages. Experiments were made below 1×10^{-4} Torr chamber pressure by operating diffusion pumps, and at as low as 1×10^{-6} Torr by operating cold shrouds. The MPD arcjet used in this experiment has the same electrical characteristics as the flight model described in the previous section, although the mass and size optimization have not been made for this model. The energy storage system, i.e. PFN, FAV driver, spark power supply, and switching devices, were contained in a pressurized vessel 60 cm in diameter and 80 cm high. The charging power supplies, control units, and gas cylinders were placed outside the chamber.

The quasisteady current-voltage characteristics of the arc discharge were found to agree with those obtained in a smaller chamber. When the arcjet was operated above the discharge current corresponding to the Alfvén critical speed,[20] it was found that the amplitude of the voltage fluctuation at 10^{-4} Torr was much smaller than that at 4×10^{-6} Torr. This difference is caused by gas entrainment into the discharge region at the higher pressure. Another feature of the voltage fluctuation is the hysteresis effect as shown in Figs. 8a and 8b, each of which was obtained from the voltage trace of a single shot at 0.24 g/s argon flow rate. Once the discharge attains a large current, as shown in Fig. 8b, the fluctuation persists even at the small current, e.g. 5 kA, whereas the fluctuation is hardly observable at the same current in Fig. 8a.

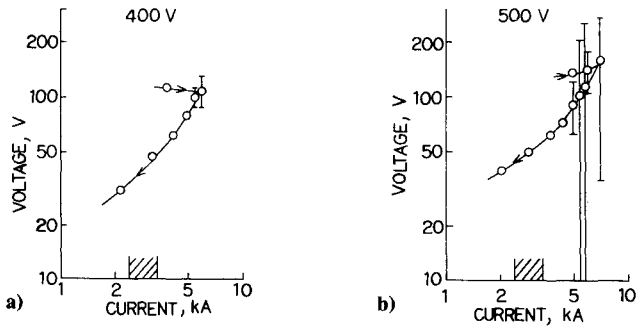

Fig. 8 Voltage current characteristics: a) 400 V charging voltage; b) 500 V charging voltage.

The plasma velocity was measured by the time-of-flight method. The ion current was monitored by a pair of Langmuir probes, one placed at 0.8 m and the other at 14 m downstream of the arcjet exit. Since the dimension of the plasma cloud was comparable to and less than the height of the chamber, the probe signal indicated the front and tail of the plasma cloud without the influence of the chamber wall. An example of ion current traces is shown in Fig. 9 for 2×10^{-5} Torr chamber pressure, 0.24 g/s argon flow rate, and 400 V charging voltage. The plasma speed was inferred from the front speed, of which the error due to the plasma expansion is less than 20%. The result is plotted against the discharge current in Fig. 10. The discharge current in this figure is the maximum value of a single run. The solid line indicated as MAX in this figure is the largest analytical prediction given by[21]

$$u = bJ^2/\dot{m} \tag{4}$$

$$b = 10^{-7}\ell n[(r_{ao}/r_c)+3/4] \tag{5}$$

in MKS units, where J is the discharge current, $\dot{m}$ is the mass flow rate, and r_{ao} and r_c are outer anode and cathode radii, respectively. The line indicated as MIN corresponds to

$$b = 10^{-7}\ell n(r_{ai}/r_c) \tag{6}$$

where r_{ai} is the inner anode radius. It is remarkable that the plasma speed exceeds the Alfv'en critical value and is close to the analytical prediction.

The arcjet and the electron gun were operated simultaneously in the floating mode to simulate the operation on the Space Shuttle pallet. The circuit diagram is illustrated in Fig. 11. The isolation resistors R_1 and R_4 are much larger than R_2 and R_3. The current path through R_1, R_2, and R_3 is strongly limited by the large resistor R_1. Other possible return circuits are a path through plasma bridge and the back reflection of the electron beam. The potential of the electron

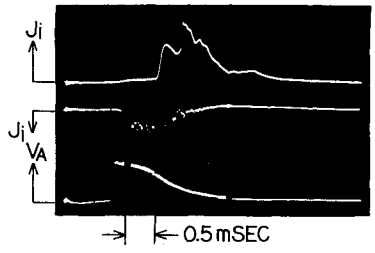

Fig. 9 Ion current traces for time-of-flight measurement.

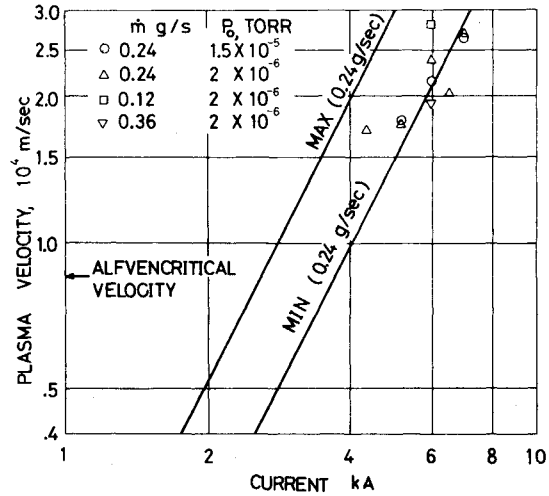

Fig. 10 Plasma velocity versus discharge current.

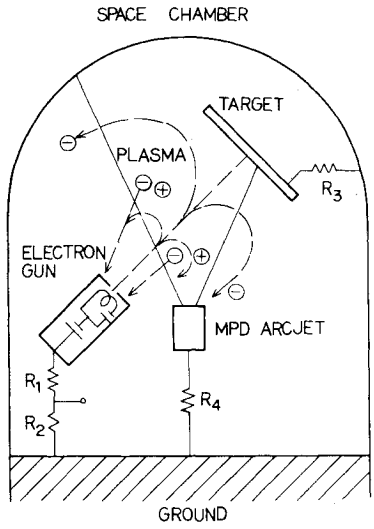

Fig. 11 Circuit diagram for charge neutralization experiment.

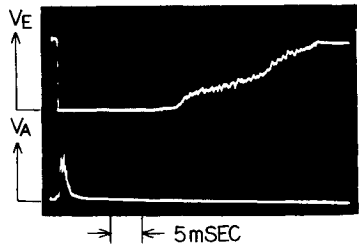

Fig. 12 Variation of electron gun anode potential with plasma injection.

gun anode was monitored by the voltage across R_2 and is shown in Fig. 12. The EBA was running in the dc mode at 500 V beam energy and 4×10^{-6} Torr chamber pressure, while the MPD arcjet was operated in a pulsed mode at 400 V charging voltage and 0.24 g/s argon flow rate. The electron gun potential, which has been at the beam acceleration voltage by the charging effect, drops to the ground potential as soon as the MPD arcjet is fired. The neutralization period is an order of magnitude longer than arcjet duration 1 ms. The neutralization period was found to range from 15 to 30 ms and to become longer as beam energy is decreased and/or the MPD arcjet charging voltage is increased. In the chamber test, the plasma lifetime or the neutralization time is strongly limited by the wall surface recombination. The wall-free condition in space may result in much longer neutralization time. The EBA operation at high power is scheduled to be made in the pulse mode synchronized with the MPD arcjet operation in order to assure the charge neutralization. Since the plasma-transit time from ground floor to ceiling of the chamber is about 1 ms, the longer neutralization time found in this experiment is attributable to the ion trapping effect discussed earlier. At the end of the neutralization period, a voltage oscillation is observed in Fig. 12. This oscillation may be related to the wave associated with the ion trapping.

Besides these results, the density distribution and hence the flow diverging angle were obtained. The MPD arcjet as well as the electron gun were safely operated with 4 m separation.

NASDA Experiment

The NASDA Space Chamber is 8.5 m in diameter and 25 m high. With the SEPAC instrument inside the chamber, the pressure was as low as 2×10^{-7} Torr. The MPD arcjet engineering model (EM) has 5 kJ capability, but the tests were made at 2 kJ. The MPD arcjet was located 2.0 m from the EBA.

During the simultaneous operation of the MPD and the EBA, the effect of beam-plasma coupling on the MPD arcjet was monitored by the anode potential of the MPD arcjet. Since the arc discharge circuit was isolated from the floating ground simulating the Shuttle pallet, it was feared that a large potential difference might appear inside the CAP container if the MPD-HD potential were to come close to the electron beam potential. The MPD anode potential was measured with and without the EBA on. The anode voltage was found to be close to the arc voltage and unaffected by the presence of the electron beam.

A TV monitor inside the chamber was found to be useful for the observation of the plasma plume, although the discharge lasts only for 1 ms. It was rather strange that the luminosity at the jet exit was observed on more than four TV frames, each representing the feature averaged for 30 ms. The long-lasting image is considered to result from the residual luminescence on the TV image tube.

In addition to the results mentioned above, measurements of electromagnetic interference (EMI) and charge neutralization were carried out. Although the boundary condition of the space chamber was not compatible with the EMI test standard, the radiation level during 1 ms slightly exceeded the Spacelab standard. The results of the charge neutralization were similar to those of JSC experiments. When the EBA was operated at full power, i.e. 7.5 kV and 1.0 A, a 10 ms neutralization period was observed for the plasma ejection by the MPD arcjet.

Conclusion

Scientific missions of the first Spacelab using an MPD arcjet were reviewed. Analytical estimation demonstrated the usefulness of an MPD arcjet plasma to neutralize an electron beam and to visualize plasma-dynamic phenomena in the ionosphere. Specifications and design criteria of the MPD arcjet were determined from the failure analysis and the mission-peculiar constraints. It was revealed by the two tests in large space chambers that the MPD arcjet was effective and safe to perform the scientific missions together with an electron beam accelerator. The test results were also informative for the MPD arcjet development as a thruster.

Acknowledgments

The author would like to express his sincere thanks to T. Obayashi, SEPAC principal investigator, University of Tokyo, for his guidance and support of this work. Thanks are extended to SEPAC members, both of the University of Tokyo and of NASA Marshall Space Flight Center for their continual cooperation.

References

[1]Obayashi, T., "Space Experiment with Particle Accelerators: SEPAC, Controlled Active Experiments in Ionosphere and Magnetosphere with Particle Accelerators on-board the Space Shuttle/Spacelab," *Report of Ionosphere and Space Research in Japan*, Vol. 30, 1976, pp. 57-68.

[2]Rudolph, L. K., Jahn, R. G., Clark, K. E., and von Jaskowsky, W. F., "Performance Characteristics of Quasi-Steady MPD Discharge," AIAA Paper 76-1000, International Electric Propulsion Conference, 1973.

[3]Krülle, G. and Zeyfang, E., "Preliminary Conclusions of Continuous Applied Field Electromagnetic Thruster Research at DFVLR," AIAA Paper 75-417, 11th Electric Propulsion Meeting, 1975.

[4]Kuriki, K., "Electric Propulsion Work in Japan," AIAA Paper 76-1066, International Electric Propulsion Conference, 1976.

[5]Parker, L. W. and Murphy, B. L., "Potential Buildup on an Electron-Emitting Ionospheric Satellite," *Journal of Geophysical Research*, Vol. 72, March 1967, pp. 1631-1636.

[6]Linson, L. M., "Current-Voltage Characteristics of an Electron-Emitting Satellite in the Ionosphere," *Journal of Geophysical Research*, Vol. 74, May 1969, pp. 2368-2375.

[7]Liemohn, H. B., "Electrical Charging of Shuttle Orbiter," BATTELLE, Pacific Northwest Laboratories, BN SA 518, 1976.

[8]Rosen, A. "Large Discharges and Arcs on Spacecraft," *Astronautics and Aeronautics*, Vol. 13, June 1975, pp. 36-44.

[9]Rosen, A. "Spacecraft Charging: Environment-Induced Anomalies," *Journal of Spacecraft and Rockets*, Vol. 13, March 1976, pp. 129-136.

[10]McPherson, D. A., Cauffman, D. P., and Schober, W. R., "Spacecraft Charging at High Altitudes: SCATHA Satellite Program," *Journal of Spacecraft and Rockets*, Vol. 12, Oct. 1975, pp. 621-626.

[11]Mirels, H. and Rosenbaum, B. M., "Analysis of One-dimensional Ion Rocket with Grid Neutralization," NASA TN D-266, 1960.

[12]Takayanagi, K., "Atomic and Molecular Processes Associated with Experiments of Particle Ejection from Space Shuttle (SEPAC Project)," *Bulletin of the ISAS, University of Tokyo*, Vol. 10, No. 2 (A), 1974 (in Japanese), pp. 753-773.

[13]Lindberg, L. and Kristferson, L., "Reverse Deflection and Contraction of a Plasma Beam Moving along Curved Magnetic Field Lines," *Cosmic Electrodynamics*, Vol. 2, Oct. 1971, pp. 305-308.

[14]Kuriki, K. and Inutake, M., "Super-Alfvénic Flow and Collision Free Shock Wave in a Plasma Wind Tunnel," *The Physics of Fluids*, Vol. 17, Jan. 1974, pp. 92-99.

[15]Kato, Y., Tajiri, M., and Taniuchi, T., "Existence Condition for Collisionless Hydromagnetic Shock Waves along the Magnetic Field," *Journal of Plasma Physics,* Vol. 6, Part 3, 1971, pp. 467-493.

[16]Schmidt, G., "Plasma Motion Across Magnetic Fields," *The Physics of Fluids*, Vol. 3, Nov. - Dec. 1960, pp. 961-965.

[17]Tidman, D. A. and Krall, N. A., *Shock Waves in Collisionless Plasmas*, John Wiley & Sons, Inc., New York, 1971, Chap. 4.

[18]Sellen, J. M., Jr. "AMPS Particle Accelerator Definition Study," TRW Systems Group, NAS 8-31375, 1975.

[19]Kuriki, K., et al., "MPD Arcjet Test in a Large Space Chamber," ISAS Research Note 33, 1977.

[20]Alfvén, H., "Collision between a Nonionized Gas and a Magnetized Plasma," *Review of Modern Physics*, Vol. 32, Oct. 1960, pp. 710-713.

[21]Jahn, R. G., *Physics of Electric Propulsion*, McGraw-Hill Inc., New York, 1968, Chap. 8.